International Journal of Automotive Technology, Vol. 5, No. 3, pp. 201−208 (2004)

1229−9138/2004/017−08

HARDWARE IN THE LOOP SIMULATION OF HYBRID VEHICLE FOR OPTIMAL ENGINE OPERATION BY CVT RATIO CONTROL

H. YEO[1)], C. H. SONG[2)], C. S. KIM[2)] and H. S. KIM[1)*]

[1)]School of Mechanical Engineering, Sungkyunkwan University, Suwon, Gyeonggi 440-746, Korea
[2)]Hyundai Motor Company, 772-1 Changduck-dong, Whasung, Gyeonggi 445-706, Korea

(Received 5 September 2003; Revised 14 February 2004)

ABSTRACT–Response characteristics of the CVT system for a parallel hybrid electric vehicle (HEV) are investigated. From the experiment, CVT ratio control algorithm for the optimal engine operation is obtained. To investigate the effect of the CVT system dynamic characteristics on the HEV performance, a hardware in the loop simulation (HILS) is performed. In the HILS, hardwares of the CVT belt-pulley and hydraulic control valves are used. It is found that the engine performance by the open loop CVT ratio control shows some deviation from the OOL in spite of the RCVs open loop control ability. To improve the engine performance, a closed loop control of the CVT ratio is proposed with variable control gains depending on the shift direction and the CVT speed ratio range by considering the nonlinear characteristics of the RCV and CVT belt-pulley dynamics. The HILS results show that the engine performance is improved by the closed loop control showing the operation trajectory close to the OOL.

KEY WORDS : HILS, HEV, CVT

1. INTRODUCTION

Next generation vehicles are under environmental and economic pressure to reduce emissions and increase fuel economy, while maintaining the same performance characteristics of present day internal combustion engine automobiles. This has prompted researchers to investigate more energy-efficient and environmentally friendly alternate powertrain technologies.

Among the alternate powertrains being investigated, hybrid electric vehicle (HEV) is considered to offer the best promise in short to midterm. The HEVs show improvements in fuel consumption and emissions with minimum extra cost. HEV drivetrains can be assigned to either the parallel hybrid or the series hybrid. In passenger car application, the parallel hybrid configuration has been used in many HEVs that come out on the market. In the parallel hybrid configuration, the mechanical connection between the components does not allow the optimization as the case in the series hybrid. However, this disadvantage can be overcome by adopting a continuously variable transmission (CVT) since CVT is able to make the engine operation run on the minimum fuel consumption region regardless of the vehicle speed.

It is well known that metal belt CVT is able to provide more efficient engine operating level by the CVT ratio control than conventional multi-ratio gearbox transmission. In the CVT ratio control, the desired CVT ratio is determined from the engine optimal operation point and the present vehicle velocity. For an ideal driving situation, this desired speed ratio is able to move the engine operation point on the optimal operation line for the minimum fuel consumption. However, there exists a response lag due to the CVT dynamics and this response lag causes a deviation between the actual engine operation point and the optimal engine operation line, which affects the HEV performance such as fuel economy.

In most simulation programs to evaluate vehicle performance, the CVT is modeled as a simple first order or second order dynamics which generates the desired speed ratio corresponding to the driver's demand. These models are good enough to evaluate the fuel economy in the initial concept design stage. However, in order to design CVT ratio control algorithm that can be implemented in prototype HEV, a detail model of the CVT is required. It is known that the metal belt CVT shows a nonlinear shift characteristics depending on the actuator pressure, rotational speed and the speed ratio (Ide, 1995). For the CVT shift dynamics, several dynamic models (Guebeli, 1992; Shafai, 1995; Song, 1998) have been proposed.

Besides the shift dynamics, dynamic characteristics of the solenoid valves, belt elasticity, and the effect of filling

**Corresponding author.* e-mail: hskim@me.skku.ac.kr

time should be considered. In the metal belt CVT system, when the upshift begins from the lowest gear ratio, the oil needs to be supplied to the primary actuator. Since the primary actuator is empty at the lowest gear ratio, there exists a filling time to fill up the empty volume of the primary actuator.

In this study, dynamic characteristics of the HEV CVT system are investigated experimentally and ratio control algorithm is obtained. Based on the ratio control algorithm, the effect of CVT system dynamics on the HEV engine operation is investigated by hardware in the loop (HIL) simulation.

2. CVT HYDRAULIC CONTROL SYSTEM

In Figure 1, hydraulic control system of the CVT used in this study is shown. The hydraulic system consists of line pressure control valve (LCV) and ratio control valve (RCV). In the LCV, the line pressure is controlled by the pitot pressure, which is proportional to the centrifugal pressure in the primary chamber. When the clutch is engaged, the primary pulley speed is equal to the engine speed. Therefore, the primary pitot pressure is directly related to the engine speed. If the engine speed increases, the pitot pressure increases and makes the spool to move to the left side, which causes to open the exhaust part. This results in the decreased line pressure. The line pressure is also controlled by the speed ratio. When the upshift occurs, the movable flange where the mechanical sensor is attached moves to the right side, which causes the cap to move to the left side by the mechanical feedback linkage which is connected to the movable flange. This gives the release of the spring compression, which moves the spool to the left side resulting in the decrease line pressure.

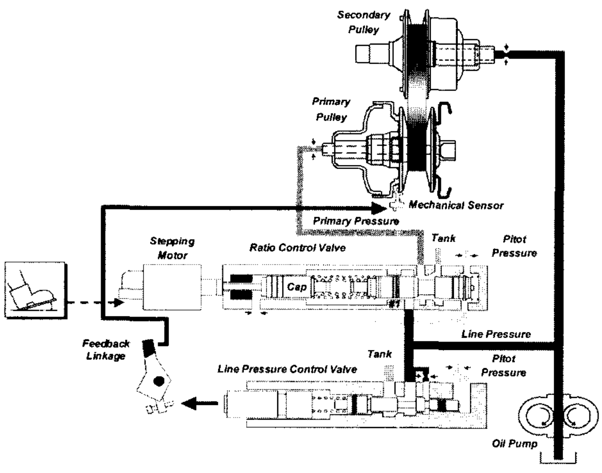

Figure 1. CVT hydraulic control system.

The RCV controls the speed ratio. When the driver pushes the drive pedal, the cap displacement increases to the right side by the stepping motor. In the meantime, the pitot pressure that is applied to the right side of the spool also increases due to the increased engine speed, which causes the spool to move to the left side. This opens the supply port #1, which results in the increased pressure of the primary actuator. Correspondingly, the belt pitch radius of the primary pulley increases due to the increased clamping force, which results in the upshift.

When the RCV spool is positioned at the threshold point where the engine pitot pressure applied to the right side of the spool is balanced with the cap compression force at the left side of the spool, the CVT ratio remains constant value. Since the cap displacement depends on the throttle valve opening (TVO), the RCV is able to control the CVT ratio according to the driver's pedal input.

In Figure 2, a detail drawing of the RCV spool is shown. Dynamic equations of the RCV spool can be derived from the force equilibrium

$$\dot{P}_{ps}=P_{pl}A_{pl}-B_{ps}\frac{P_{ps}}{M_{ps}}-K_{ps2}(x_{ps}+x_{pso}+x_{pc})$$
$$+K_{ps1}(x_{ps10}-x_{ps})-k_{ps3}(x_{ps}+x_{pc}-X_0) \quad (1)$$

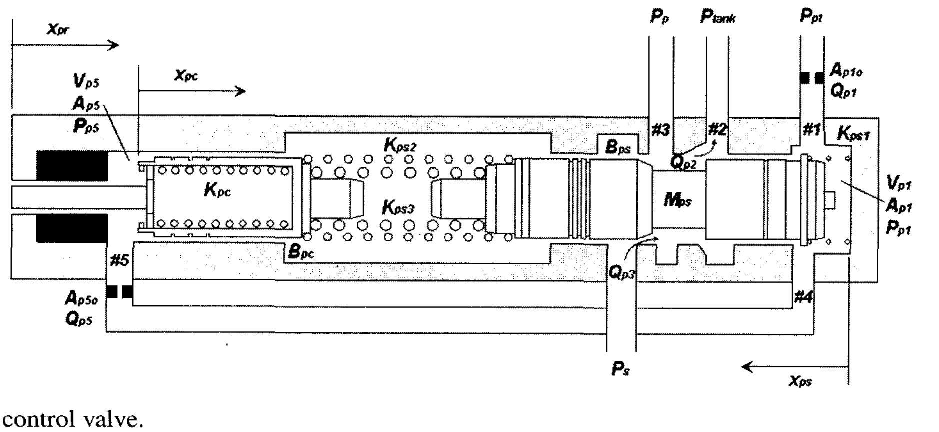

Figure 2. Ratio control valve.

where P_{ps} is the linear momentum of the primary valve spool, A_{pl} is the land area, B_{ps} is the damping coefficient, M_{ps} is the spool mass, K_{ps2}, K_{ps1} and k_{pss} are the spring stiffness, P_{pl} is the pitot pressure applied to the right side of the spool.

3. EXPERIMENTAL INVESTIGATION OF RESPONSE LAG AND RATIO CONTROL ALGORITHM FOR HEV CVT

The CVT ratio should be controlled to move the engine operation point on the optimal operation line (OOL). However, the CVT has a response lag which may cause a deviation of the engine operation from the OOL. The CVT response lag results from the dynamic characteristics of the hydraulic control valve and belt-pulley mechanics. In this study, the response characteristics of the CVT are investigated by experiments. In order to obtain the response characteristics of the CVT itself, the CVT system should be separated from the engine and the drivetrain. Since the engine pitot pressure, TVO and the speed ratio are required as the inputs to the CVT system, these input variables are simulated using the proportional valve and the stepping motors. In Figure 3, the LCV and RCV with the input simulators are shown.

The LCV controls the line pressure depending on the engine pitot pressure and the CVT ratio. The engine pitot pressure is simulated by the proportional valve which generates the pitot pressure corresponding to the engine speed. The spring compression by the CVT ratio feedback linkage is simulated by the stepping motor. The input variables of the RCV are simulated in a similar manner. In the RCV, the engine pitot pressure and the TVO are used as the input variables to control the flow to the primary actuator. These input variables are simulated using the proportional valve and stepping motor as shown in Figure 3(b). Using the LCV and RCV in Figure 3, response characteristics of the CVT are investigated. In Figure 4, experimental results of the CVT response are shown. In the experiment, upshift is carried out from the lowest gear ratio, i=2.47 by applying the stepwise pitot pressure which corresponds to the engine speed ω_e=1800 rpm. The line pressure is maintained constant as P_s=19 bar. The input signal was applied at point A to generate the pitot pressure. When the stepwise pitot pressure is applied, the RCV spool moves to the left side, which allows the supply port to be open. This results in the pressure increase in the primary actuator, and the upshift is carried out. The primary pressure builds up after some time delay. The line pressure decreases slightly after some time delay and recovers the target line pressure. The reduction of the line pressure is due to the shortage of the oil supply which is required to fill up the primary actuator volume, that is empty at the lowest gear ratio i=2.47. From the experimental results, it is seen that the primary pressure reaches its peak valve at the point B where the upshift begins and the filling time is measured from the point A to the point B as 300 msec. But, since experiments are performed with the test rig, this result includes the effect of the hydraulic line volume, the

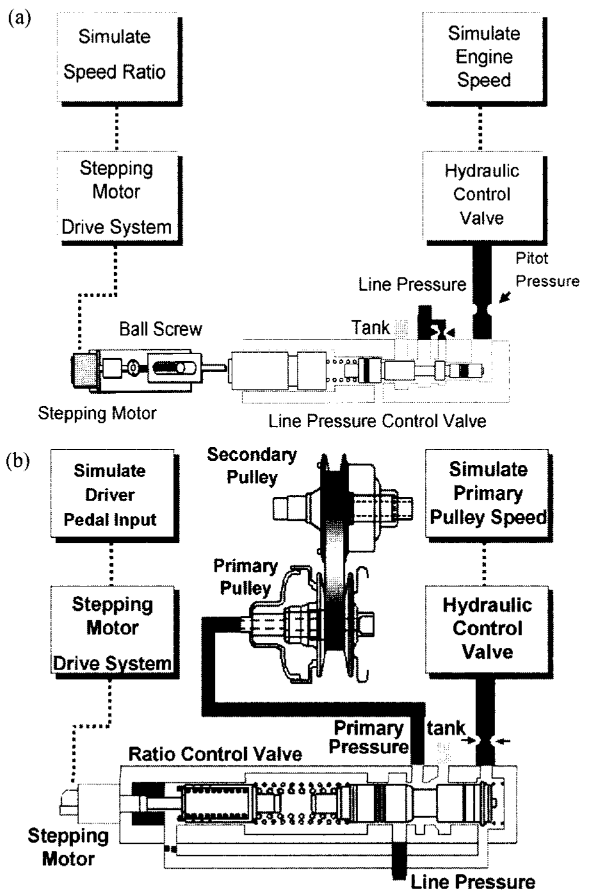

Figure 3. (a) LCV and (b) RCV with input simulator.

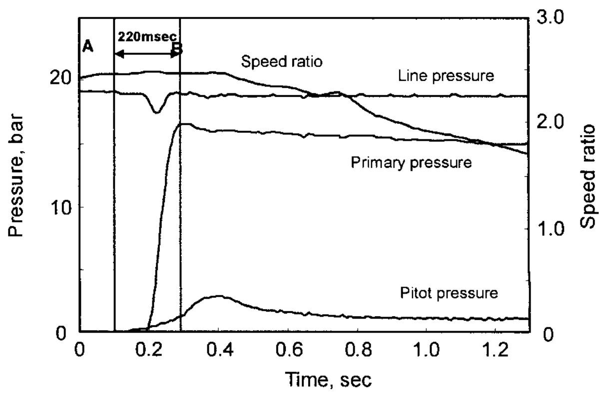

Figure 4. Time response of CVT ratio at upshift.

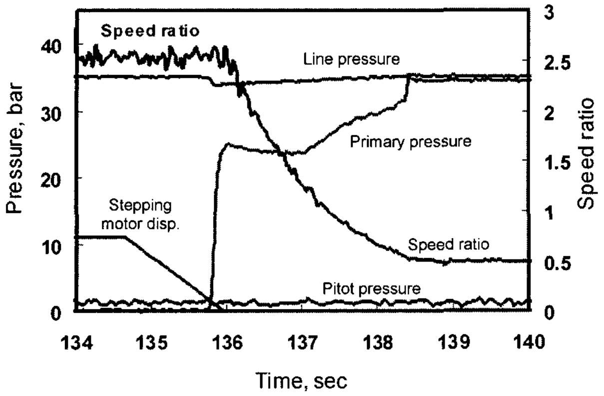

Figure 5. Transient response of CVT ratio control system for upshift at 2000 rpm.

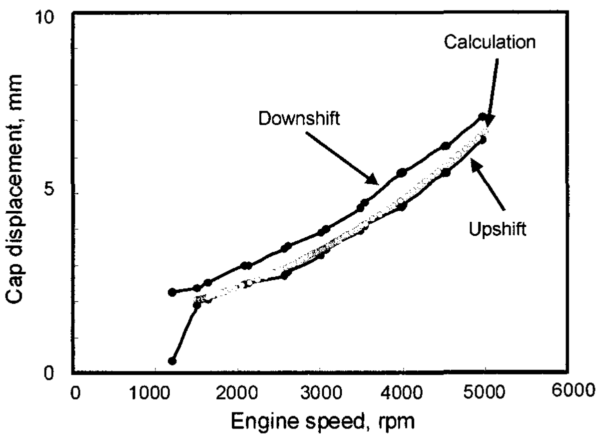

Figure 6. Cap displacement vs. engine speed.

proportional control valve dynamics, etc. Therefore, the response delay due to the filling time when the upshift begins from the lowest gear ratio is estimated at about 200~250 msec.

In Figure 5, experimental results of the primary pressure, line pressure, pitot pressure and the CVT ratio are plotted for the cap displacement input. As shown in Figure 5, the primary pressure begins to increase when the cap displacement approaches closely to the minimum position. The upshift begins after some time delay. Once the upshift begins, the primary pressure decreases slightly and increases again until the upshift is finished. The pressure decrease is due to the oil flow to the primary actuator since the primary actuator volume increases as the upshift progresses.

It is seen from Figure 5 that the shift point is directly related with the magnitude of the cap displacement and the pitot pressure, i.e., the engine speed. In Figure 6, experimental results for the cap position where the shift begins are plotted with respect to the engine speed. In addition, calculated cap position from Equation (1) is

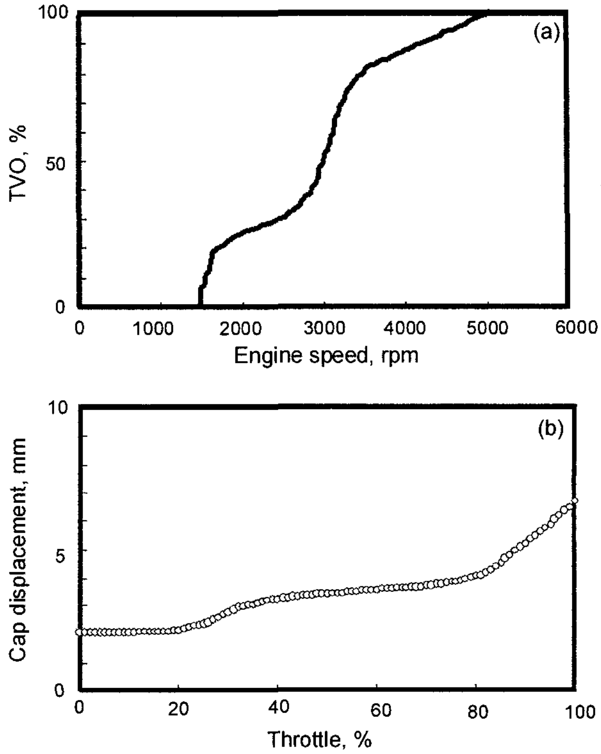

Figure 7. (a) Throttle vs. engine speed by OOL and (b) cap displacement vs. throttle.

compared with the experimental results. In the calculation, the cap displacement is obtained at a steady state for the given engine pitot pressure, i.e., the engine speed. As shown in Figure 6, the cap position where the shift begins depends on the engine speed. It is noted that as the cap displacement becomes larger, the higher engine speed is required for the shift. The means that if we set up the cap displacement related with the TVO, an optimal engine operation can be achieved. However, as shown in Figure 6, there exists a hysteresis in the cap displacement between the upshift and the downshift. This hysteresis is considered to be the effect of the nonlinearity inherent to the CVT system and may cause a deviation of the engine operation from the OOL.

Figure 7 shows the relationship between the cap displacement and the TVO. In Figure 7(a), the optimal engine speed can be determined from the OOL for various TVOs. Since the TVO is directly related with the optimal engine speed, the cap displacement vs. TVO plot can be redrawn as shown in Figure 7(b). Therefore, if we control the stepping motor according to the driver's input, i.e., the TVO input, the optimal engine operation can be obtained, which means that the CVT ratio control can be realized in a open loop control. In other words, if we store the relationship of the cap displacement vs. TVO in the transmission control unit, an optimal engine operation can be achieved by the CVT ratio control regardless of the vehicle velocity.

4. HARDWARE IN THE LOOP SIMULATION OF HEV FOR OPTIMAL ENGINE OPERATION

As shown in the experimental results in Figure 4~Figure 6, the CVT system shows nonlinear behavior due to the response lag, belt-pulley mechanics, hysteresis of the RCV and the inherent nonlinear characteristics of the hydraulic control valves. Therefore, in this study, in order to investigate the effect of the CVT system on the HEV performance, hardware in the loop (HIL) simulation is performed. In Figure 8, a schematic diagram of the HEV CVT HILS system is shown. The HIL simulator, shown in Figure 8 consists of a hardware part, software part and input/output (I/O) part. The hardware part is composed of CVT belt-pulley, hydraulic control valves, digital signal processor, host computer. The CVT system is driven by the motor. The LCV and RCV are controlled using the test rig in Figure 3.

The dynamic models of the HEV powertrain such as engine, motor and battery are obtained with MATLAB simulink and are used as the software part of the HIL simulator. A/D and D/A converters for data communication between the hardware and software parts are in the I/O part.

4.1. Hardware Part

Figure 8 shows the hardwares which includes the CVT belt-pulley, LCV and RCV. A DS1103 controller board is used as a signal processor, the DSP board has a 400 MHz main processor, 2 Mbyte local SRAM, 32 Mbyte global DRAM. The HILS is performed by linking the HEV simulator that is code generated to realize to real time simulator to the DSP.

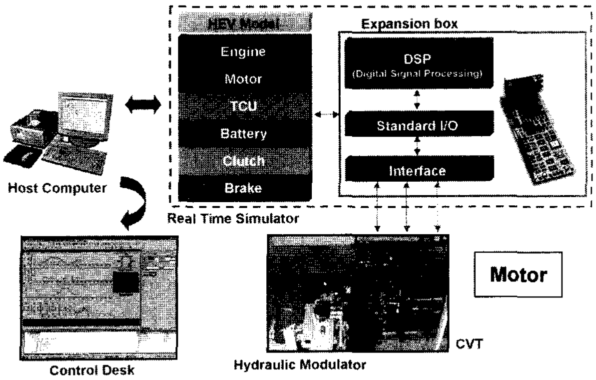

Figure 8. HILS system.

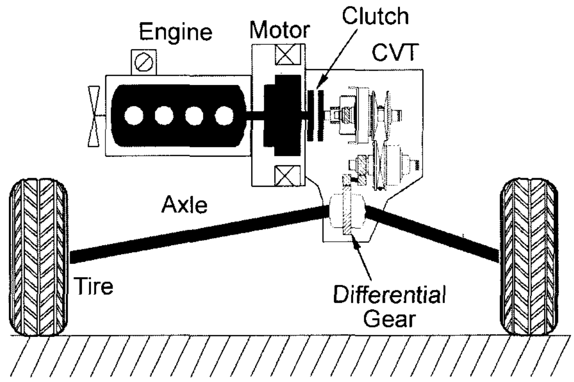

Figure 9. Schematic diagram of parallel HEV.

4.2. Software Part

The software part of the HEV CVT simulator is mainly composed of the vehicle dynamic model and the experimental conditions. Dynamic modeling of the HEV powertrain are explained in this section. Figure 9 shows a schematic diagram of the parallel HEV used in this study. Engine is connected with a motor by a single shaft. One clutch is used between the motor and the transmission. As a transmission, a metal belt CVT is used to maintain the engine operation on the minimum fuel consumption region independent of the vehicle speed.

4.2.1. Vehicle dynamics

Equation of motion of the HEV when the engine and the motor work together is represented as

$$\frac{dV}{dt}=\frac{\eta_T\eta_D i\frac{N}{R_t}(T_e+T_m-T_{LOSS})-F_L-F_b-\eta_T\eta_D\frac{N^2 i\frac{di}{dt}J}{R_t^2}V}{M+\frac{J_w}{R_t^2}+\eta_T\eta_D\left(\frac{iN}{R_t}\right)^2 J} \quad (2)$$

where T_e is the engine torque, T_m is the motor torque, F_L is the road load, F_b is the brake force, R_t is the tire radius, M is the vehicle mass, η_T is CVT efficiency, η_D is final reduction gear efficiency, and J is the equivalent inertia of the engine and clutch.

4.1.2. Engine

Since the engine and the motor is connected, dynamic equation of the engine is expressed as

$$(J_e+J_m)\frac{J\omega_e}{dt}=T_e+T_m-T_{loss}-T_{net} \quad (3)$$

where J_e, J_m are the engine and the motor inertia, respectively. ω_e is the engine speed, T_{loss} is the auxiliary device loss, T_{net} is the CVT input torque.

4.1.3. Motor

The motor is used as a tractive effort when the battery is discharged and is used as a generator when the battery is charged, in other words, in the regenerative braking mode. When the motor is used as a tractive effort, the motor torque T_m is represented as

$$T_m = K_t I \quad (4)$$

where K_t is the motor torque constant, and I is the current. The motor torque transmitted to the wheel can be obtained including the motor efficiency.

4.1.4. Battery

The battery SOC is represented as follows

$$SOC = SOC_0 - \frac{B_c \Delta t}{3600 B_F} \quad (5)$$

where SOC_0 is the battery initial $SOC[\%]$, B_c is the consumed power [kW], B_F is the full charge power [kW], and Δt is the sampling time. In charging or discharging process, the inner resistance of the battery changes depending on the battery SOC. This resistance change is considered as an efficiency map.

4.3. HEV Operation Algorithm

For the HEV operation, the operation algorithm is required. A variety of the operation algorithms can be used depending on the HEV structure, motor capacity, etc. For the HEV used in this study, the power assist algorithm is used, in which the motor is used to assist the engine while the engine propels the vehicle as a primary power source. The power assist algorithm used in this study consists of 3 driving modes; acceleration, normal and deceleration mode. The power assist of the electric motor is applied in the acceleration mode when the HEV requires high power. In the normal mode, where the vehicle runs in a slight acceleration, the engine only propels the vehicle since the required power is not large. When the vehicle runs in deceleration, the regenerative braking is performed to recuperative the vehicle kinetic energy, which recovers the battery state of charge (SOC).

Table 1. Vehicle data.

Engine stroke volume	1600 cc
Engine maximum torque	140 Nm
Motor torque at 0 rpm	50 Nm
Motor Peak power	10 kW
CVT gear ratio range	0.455~2.47
Final reduction gear ratio	5.763
Vehicle mass	1380 kg
Front project area	1.964 m^2
Drag coefficient	0.346
Tire radius	0.279 m

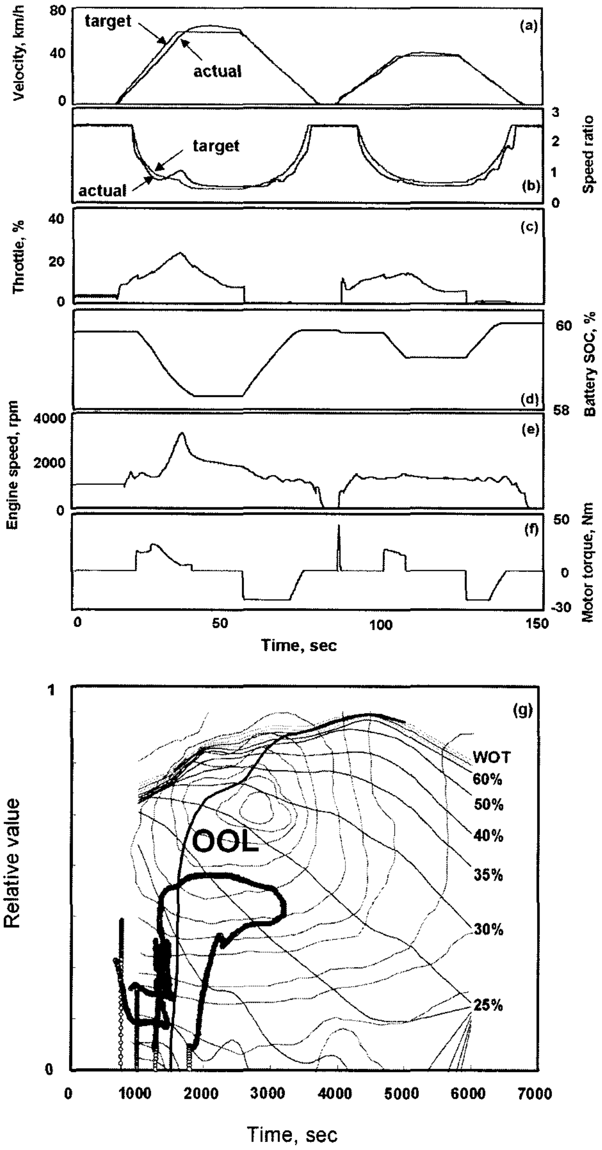

Figure 10. HILS results for open loop control.

5. RESULTS AND DISCUSSION

In the HILS, the drive pedal and the brake pedal are operated by the driver model inserted in the simulator to follow the reference driving schedule. Hybrid control unit (HCU) calculates the TVO, target motor torque and the CVT ratio depending on the HEV operation mode. The line pressure is controlled at the LCV according to the pitot pressure and CVT ratio simulated by the proportional valve and the stepping motor. The RCV controls the CVT ratio depending on the TVO and the engine speed. In Table 1, vehicle data used in the HILS are shown.

In the HILS, the engine performance by the open loop

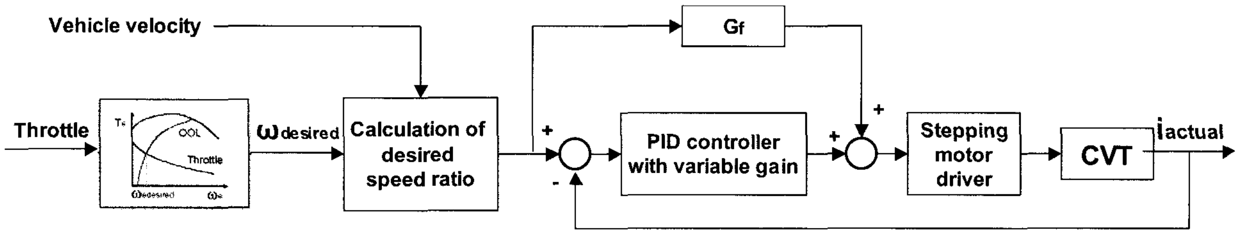

Figure 11. Closed loop control.

control is investigated. In Figure 10, the HILS results by the open loop CVT ratio control are shown. The actual vehicle velocity (a) follows the target velocity closely.

The CVT ratio (b) follows the target ratio in the acceleration and deceleration mode, but shows some difference. The difference between the actual ratio and target ratio is due to the RCV characteristics. As shown in Figure 6, the cap displacement has a hysteresis characteristic, which causes a deviation in following the target ratio. The CVT ratio shows the upshift and downshift corresponding to the engine speed change (e) rather than the TVO input in the first acceleration mode. This can be explained by the RCV characteristics. As shown in Figure 7(b), the cap displacement does not change much until the TVO increases up to 20%. Therefore, the RCV determines the CVT ratio mainly depending on the engine speed instead of the TVO change in the relatively small TVO range, which results in the upshift and downshift behavior of the CVT ratio following the engine speed. The battery SOC (d) decreases when the motor is used to assist the engine to propel the vehicle and increases when the motor is used as a generator in the regenerative braking mode. The motor torque (f) shows a positive value when the motor is used to assist the engine and shows a negative value when it is used as a generator in the regenerative braking. The regenerative motor torque is limited to 25 Nm in this study. In Figure 10(g), the engine operation trajectory is shown. It is seen that even if the overall trend of the engine operation trajectory follows the OOL, the engine is operated out of the OOL for the engine speed, ω_e=2000~3000 rpm, which is considered to be the effect of the RCV characteristics.

From the HILS results, it is found that even if the RCV used in this study is designed to provide the optimal CVT ratio with respect to the drive pedal opening and engine speed, the open loop control of the CVT ratio does not provide a satisfactory engine performance. Therefore, in this study, a closed loop control of the CVT ratio is designed. In the closed loop control, PID control logic with variable gains is proposed by considering the nonlinear characteristics of the RCV and CVT belt-pulley dynamics. In Table 2, control gain of the PID logic is shown. As shown in Table 2, different control gains are used depending on the shift direction and the speed ratio range.

Table 2. PID control gain.

	$0.455 < i \leq 1$	$1 < i < 2.47$
Upshift	K_{P1}, K_{I1}, K_{D1}	K_{P2}, K_{I2}, K_{D2}
Downshift	K_{P3}, K_{I3}, K_{D3}	K_{P4}, K_{I4}, K_{D4}

In Figure 11, a block diagram of the CVT ratio closed loop control is shown. The desired CVT ratio is determined from the OOL corresponding to the driver pedal opening, i.e., the TVO input and the vehicle velocity. The actual speed ratio is obtained by measuring the primary and secondary pulley speed and feedbacked to be compared with the target ratio. A feed forward control is added to improve the robustness to the disturbance.

Figure 12 shows the HILS results by the closed loop CVT ratio control. The actual vehicle velocity(a) follows the reference driving schedule closely. It is seen from Figure 12(b) that the tracking performance of the CVT ratio by the closed loop control is improved much compared to that of the open loop control. The battery SOC (d) and the motor torque (f) show similar responses with those by the open loop control. The engine speed (e) changes corresponding to the TVO (c) input. It is noted that the maximum engine speed is decreased due to the improved CVT ratio control. It is seen from Figure 12(g) that the engine performance is improved by the closed loop control showing the operation trajectory near to the OOL.

To investigate the engine performance by the closed loop control, the engine operation trajectory is compared using the following RMS(root mean square) equation

$$RMS=\sqrt{\frac{\sum_{i=1}^{N}\left[\left(\frac{T_i-T_o}{C_1}\right)^2+\left(\frac{\omega_i-\omega_o}{C_2}\right)^2\right]}{N}} \tag{6}$$

where (T_i, ω_i) is the engine torque and speed at ith time step, (T_o, ω_o) is the optimal engine torque and speed for a given throttle valve opening at ith time step, C1, C2 are

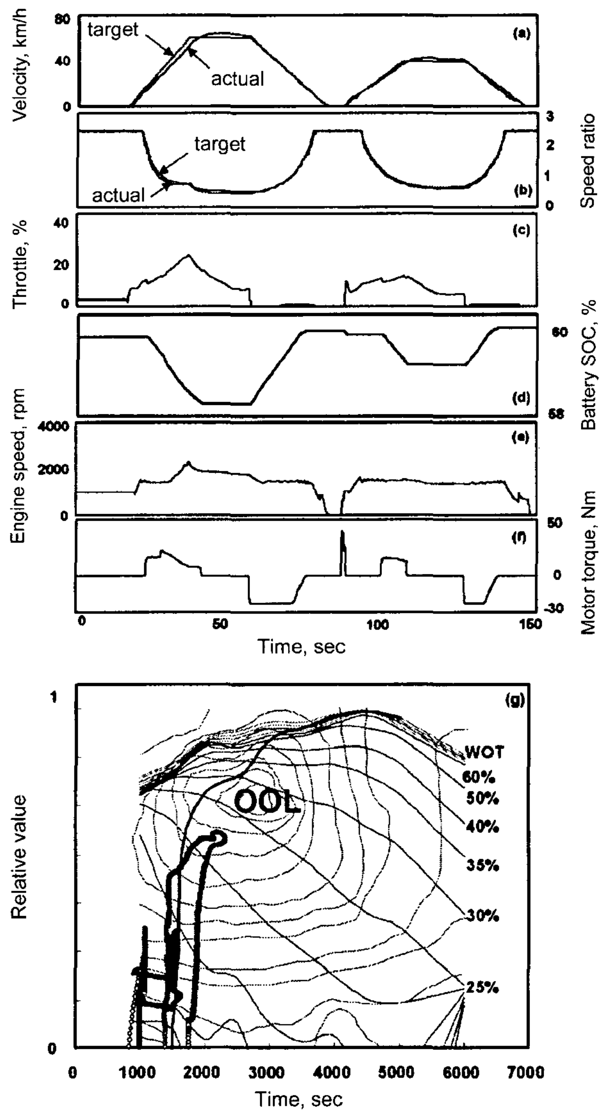

Figure 12. HILS results for closed loop control.

the scaling factor, N is the total number of calculation used in the simulation. Equation (6) indicates how closely the engine operation is carried out near the OOL. From Equation (6), it is found that RMS of the closed loop control is 0.44 while RMS of the open loop control is 0.58, which demonstrates the improvement of the engine operation by the closed loop control.

Even if the closed loop CVT control gives the improved engine operation performance on the OOL, it is noted that there still exists some deviation from the OOL. This deviation is considered to be the effect of the response of the CVT system such as time lag, etc. as explained previously.

6. CONCLUSION

Response characteristics of the CVT system for a parallel hybrid electric vehicle (HEV) are investigated. From the experiment, CVT ratio control algorithm for the optimal engine operation is obtained. It is found that the optimal engine operation can be achieved in open loop manner by relating the RCT spool position to the TVO input corresponding to the desired engine speed. To investigate the effect of the CVT system dynamic characteristics on the HEV performance, a hardware in the loop simulation (HILS) is performed. In the HILS, hardwares of the CVT belt-pulley and hydraulic control valves are used. It is found that the engine performance by the open loop CVT ratio control shows some deviation from the OOL in spite of the RCVs open loop control ability. To improve the engine performance, a closed loop control of the CVT ratio is proposed. In the closed loop control, variable control gains are used depending on the shift direction and the CVT speed ratio range by considering the nonlinear characteristics of the RCV and CV0T belt-pulley dynamics. The HILS results show that the engine performance is improved by the closed loop control showing the operation trajectory close to the OOL.

ACKNOWLEDGEMENT–The authors are grateful for the support provided by a grant from the Hyundai Motor Company. Also this work was supported by the Brain Korea project in 2003.

REFERENCES

Gueblei, M. Micklem, J. D. and Burrows, C. R. (1992). Maximum transmission efficiency of a steel belt continuously variable transmission. *Trans. of the ASME, Journel. of Mechanical Design* **115**, 1044–1048.

Ide, T., Udagawa, A. and Kataoka, R. (1995). Simulation approach to the effect of the ratio changing speed of a metal V-belt CVT on the vehicle response. *Int. J. of Vehicle System Dynamics* **24**, 377–388.

Shafai, E., Simons, M. Neff, U. and Geering, H. P. (1995). Model of a continuously variable transmission. *In Proc. of the 1st IFAC Workshop on Advances in Automotive Control* 99–107.

Song, H., Kim, J. and Kim, H. (1998). Dynamic response of metal belt CVT vehicle and electronic control of shift ratio. *KSME International Journal* **22,** 738–747.